Continuous atom laser with Bose–Einstein condensates involving three-body interactions

2010 J. Phys. B: At. Mol. Opt. Phys. 43 105302

(http://iopscience.iop.org/0953-4075/43/10/105302)

J. Phys. B: At. Mol. Opt. Phys. **43** (2010) 105302 (6pp) doi:10.1088/0953-4075/43/10/105302

Continuous atom laser with Bose–Einstein condensates involving three-body interactions

A V Carpentier[1], H Michinel[1], D N Olivieri[2] and D Novoa[1]

[1] Área de Óptica, Facultade de Ciencias de Ourense, Universidade de Vigo, As Lagoas s/n, Ourense, ES-32004, Spain
[2] Área de Linguaxes e sistemas informáticos, Escola Superior de Enxeñería Informática, Universidade de Vigo, As Lagoas s/n, Ourense, ES-32004, Spain

E-mail: avcarpentier@uvigo.es

Received 23 December 2009, in final form 30 March 2010
Published 26 April 2010
Online at stacks.iop.org/JPhysB/43/105302

Abstract
We demonstrate, through numerical simulations, the emission of a coherent continuous matter wave of constant amplitude from a Bose–Einstein condensate in a shallow optical dipole trap. The process is achieved by spatial control of the variations of the scattering length along the trapping axis, including elastic three-body interactions due to dipole interactions. In our approach, the outcoupling mechanism is atomic interactions, and thus, the trap remains unaltered. We calculate analytically the parameters for the experimental implementation of this continuous wave atom laser.

(Some figures in this article are in colour only in the electronic version)

1. Introduction

The experimental realization of Bose–Einstein condensates (BECs) with alkali atoms [1] has opened the door to the realization of atomic beam sources of high coherence and brightness, with strong analogy to optical laser beams. Such 'atom lasers' promise unprecedented achievements in fields such as atomic interferometry or gravimetry and have been proposed in several configurations, predominantly pulsed [2–4] or semicontinuous [5–9], and with different outcoupling mechanisms for guided atom lasers [10–12] and free-falling atom lasers [13].

For instance, the first atom laser used short radio-frequency pulses to outcouple atoms from the cavity, flipping the spins of some of the atoms and releasing them from the trap with the aid of gravity [2]. However, despite its success in the first experiments on atom laser operation, spin-flipping techniques have some limitations as a versatile outcoupling mechanism for coherent matter-wave sources. In first place, there are strong fluctuations in the output at high fluxes due to the fact that the spin-flipping mechanism populates all accessible Zeeman states [14]. This constitutes a strong drawback for practical applications of atom lasers in high-precision measurements such as matter-wave gyroscopes [15]. Moreover, in the former atom lasers, the emission process is driven by gravity and thus the resulting matter wave is always emitted in the vertical direction.

Atomic soliton lasers overcome the previous limitations using the mechanism of modulational instability to trigger the outcoupling of atoms from the cloud [3, 4]. Thus, in this case, there is no need for gravity since the emission is obtained by an adequate combination of nonlinear effects in the atom cloud and the manipulation of the trap. In particular, the necessary condition is that the total number of particles in the cloud exceeds a critical threshold. Therefore, atomic soliton lasers add arbitrary directionality to the emitted beam. However, currently proposed matter-wave sources based on nonlinear effects can only operate in a pulsed regime due to modulational instability of the beam: a nonlinear effect which yields a burst of atomic solitons [16–18]. These *localized* nonlinear waves arise as a result of the perfect balance between dispersive and nonlinear effects in one-dimensional systems. A set of robust pulses that propagate without shape distortion is therefore produced after the emission, thereby precluding continuous operation of the matter-wave laser.

The goal of this paper is to present a novel outcoupling mechanism for atomic beam sources which overcomes all the

previous problems and produces directional continuous wave (CW) emission of an atomic beam with constant amplitude. The trick is to use a combination of a shallow dipolar potential with attractive two-body and repulsive three-body interactions. Such interatomic potentials can be obtained for strongly dipolar atomic systems in the presence of adequately tuned magnetic fields. [19] We will show that this technique allows both the ability to extract atoms from the trap [4] and to overcome modulational instability of the outcoupled beam, thus providing fluent CW operation of the matter-wave laser. Moreover, we will show that because of the inclusion of the three-body elastic repulsion, the emitted wave displays a constant amplitude and is very robust against perturbations, permitting the achievement of atomic coherent sources with unprecedented brightness and stability.

2. System configuration and theoretical model

Let us assume that an elongated BEC is strongly trapped in the transverse directions (x, y) by a parabolic potential $V_\perp$ and weakly confined in the longitudinal axis z by a shallow dipole trap V_z of width L and depth V_0. We also assume a step variation along z of the atomic interactions. Thus, for $z < 0$ (where the condensate is initially placed at $t = 0$), the interatomic forces are set to a negligible value, whereas in the $z \geqslant 0$ region, the value of the scattering length is such as to yield strong two-body and three-body interactions comparable to the trapping force along z.

We will consider the case of both two-body attractive and three-body repulsive forces in the region $z \geqslant 0$. The techniques for controlling the scattering length which produces two-body attractive interactions are well known and may include optical or magnetic fields [18, 20, 21]. It has also been proposed that *repulsive* three-body forces can be activated with an optical lattice driven by microwave fields in ultracold gases of highly polar molecules [19], such as RbCs [22] or atoms like Cr [23]. For this technique, Hubbard models predict strong nearest-neighbour three-body interactions, whereas the two-body terms can be tuned independently. Also, recent experiments with ultracold Cs atoms [24] have revealed the existence of the so-called Efimov states, which represent a paradigm for universal quantum states in the three-body sector. These remarkable results have opened the possibility of novel BEC applications based on three-body controlled interactions, as presented in this paper.

We will consider here a system of N weakly interacting dipole bosons of mass m, trapped in a potential $V(\vec{r})$, where the evolution in time t of the condensate wavefunction Ψ is correctly described according to experiments in [25] by a mean field Gross–Pitaevskii equation of the form

$$i\hbar\frac{\partial\Psi}{\partial t} = -\frac{\hbar^2}{2m}\nabla^2\Psi + V(\vec{r})\Psi + \Delta(z, |\Psi|^2)\Psi, \qquad (1)$$

where $N = \int |\Psi|^2 \, d^3\mathbf{r}$. The functions V and Δ describe respectively the external trap and the dipole–dipole induced potential, which can be activated in the region $z > 0$. In this work we consider a cigar-shaped BEC which is tightly confined in (x, y) by means of a tubular harmonic trap. A *shallow* potential provided by an optical dipole trap V_z [26, 27] keeps the cloud trapped along the z direction. Thus, the explicit form of the three-dimensional trap V is given by

$$V(\vec{r}) = V_\perp + V_z = \frac{m\nu_\perp^2}{2}(x^2 + y^2) + V_0(z/L), \qquad (2)$$

$\nu_\perp$ being the frequency of the parabolic trap, V_0 the depth of the shallow optical dipole potential and L the characteristic size. The potential barrier can be overcome, *without destroying it*, if there is a spatial variation of atomic interactions. Thus, we will consider the simple case in which the last term of equation (2) is modulated by a step function along z of the form $\Delta(z < 0) = 0$ and $\Delta(z \geqslant 0) = U_2|\Psi|^2 - U_3|\Psi|^4$ indicating $U_2 = 4\pi\hbar^2 a/m$ and $U_3 = U_2 b$ as the strength of two-body and three-body interactions, respectively. The previous energies are determined by the value of the s-wave scattering length a and an effective volume parameter b, which indicate that three-body interactions act in a range $\approx b^{1/3}$. In the present work, we will consider a and b as positive constants.

3. One-dimensional eigenstates

We will consider setups in which the ground state of the optical dipole trap is much larger than the ground state of the transverse harmonic potential. In this situation, we can describe the dynamics of the condensate in the quasi-one-dimensional limit as given by a factorized wavefunction of the form [16, 28] $\Psi(\mathbf{r}, t) = \Phi_0(x, y) \cdot \chi(z, t)$. The density of atoms per unit length is given by $|\chi|^2$. Normalizing the squared wavefunction by setting $|\psi|^2 = \sqrt{8}\pi a|\chi|^2$, the following dimensionless equation is obtained:

$$i\frac{\partial\psi}{\partial\tau} = -\frac{1}{2}\frac{\partial^2\psi}{\partial\eta^2} + f(\eta)\psi + (\alpha|\psi|^2 - \beta|\psi|^4)\psi, \qquad (3)$$

where the normalized variables in time and space are $\tau = \nu_\perp t$ (time measured in units of the inverse of the radial trapping frequency) and $\eta = z/r_\perp$ (length expressed in units of the transverse size of the cloud $r_\perp = \sqrt{\hbar/m\nu_\perp}$), $f(\eta) = 2V_z/\hbar\nu_\perp$, and α and $\beta = b/4\sqrt{2}ar_\perp^2$ are the effective trap two-body and three-body atomic interaction coefficients. Equation (3) is known as the cubic–quintic (CQ) nonlinear Schrödinger equation due to its dependence upon the cubic and quintic powers of the wavefunction. This model has been extensively used in nonlinear optics [29] as well as in superfluidity [30] and has known analytical solutions for the one-dimensional case.

In figure 1, the geometry of the system to be considered in this paper is shown. The shallow potential with depth V_0 and width L is represented by the shaded region. Within the zone $\eta \geqslant 0$, non-zero interatomic interactions can be achieved by magnetically tuning the Feshbach resonances [18, 20] or by optical manipulation [19, 21].

We have searched numerically for eigenstates of equation (3) with the form $\psi(\eta, \tau) = \phi(\eta)\, e^{i\mu\tau}$, where μ is the chemical potential. It is well known that equation (3) features a cut-off in the chemical potential spectrum, $\mu_{cr} = \frac{3\alpha^2}{16\beta}$, which constitutes the upper border of the existence domain of localized solitonic solutions [30].

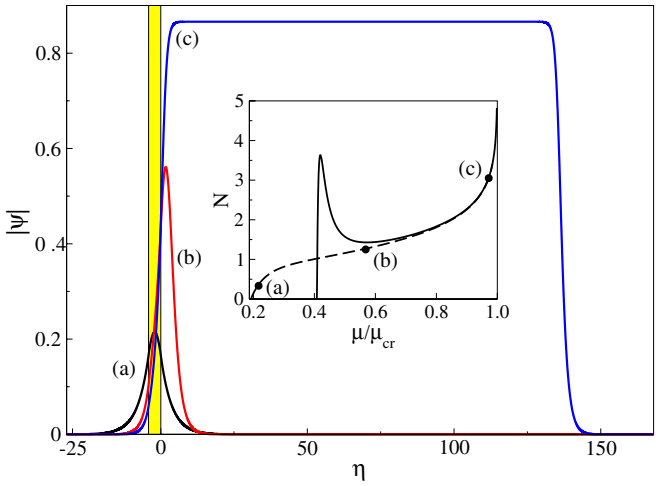

Figure 1. Amplitude profiles of several eigenstates of equation (3) calculated for different numbers of atoms in the cloud. The right edge of the shallow trap (shaded zone) is located at $\eta = 0$. For the zone with $\eta > 0$, both attractive two-body and repulsive three-body interactions are characterized by $\alpha = \beta = 1$. Inset: dependence of the number of particles in the condensate N on the chemical potential μ/μ_{cr}. The dashed (solid) line corresponds to the system displayed in the outer plot with a potential of width L ($L' = 4L$)). The labelled points refer to the eigenfunctions displayed.

Starting from the ground state of the trapping potential ((a) in figure 1) and by increasing gradually the number of atoms N, the eigenfunctions tend to enter the nonlinear zone ((b) in figure 1) displaying a high spatial localization. Once N reaches a certain critical value, the shape of the eigenstate approaches that of a continuous beam of fixed amplitude located outside the trap ((c) in figure 1). In the latter case, the value of the amplitude A is completely determined by the strength of the atomic interactions and can be easily calculated for a plane wave solution of the CQ homogeneous model [30].

As it can be appreciated in the inset of figure 1, in the case of a narrow trap of width L, the dashed curve N versus μ/μ_{cr} monotonically increases (far enough from the critical value μ_{cr} where it becomes divergent) indicating that all eigenstates are stable. Otherwise, the solid curve corresponding to a system with a trap of width $L' = 4L$ shows a region with a negative slope, yielding to the existence of an unstable domain. Note that for $\mu \to \mu_{cr}$, both curves merge because the nonlinearity overcomes the trapping potential.

4. Continuous wave emission

Taking into account the previous eigenstate structure of equation (3), we have performed a systematic analysis of the evolution dynamics of an initial Gaussian atomic cloud of unit amplitude and width $\omega = 5$ placed at the centre of a shallow square trap of depth $V_0 = 0.09$ and width $L = 4$, by means of numerical simulations of equation (3) in different parametric regimes. Subsequent feeding of the cloud with more atoms [31] has been simulated by adding a linear gain term $i\Gamma\psi$ to equation (3) ($\Gamma \in \Re$) localized in the trapping region. In the absence of nonlinear interactions ($\alpha = \beta = 0$), the gain effect is to increase the density of atoms in the trap. When only two-body interactions are considered ($\beta = 0$), a burst of solitons is emitted towards the region $\eta > 0$ as predicted in previous work [4] (see picture (a) in figure 2). When $\beta > 0$ and Γ is set below a certain critical threshold Γ_{cr}, which

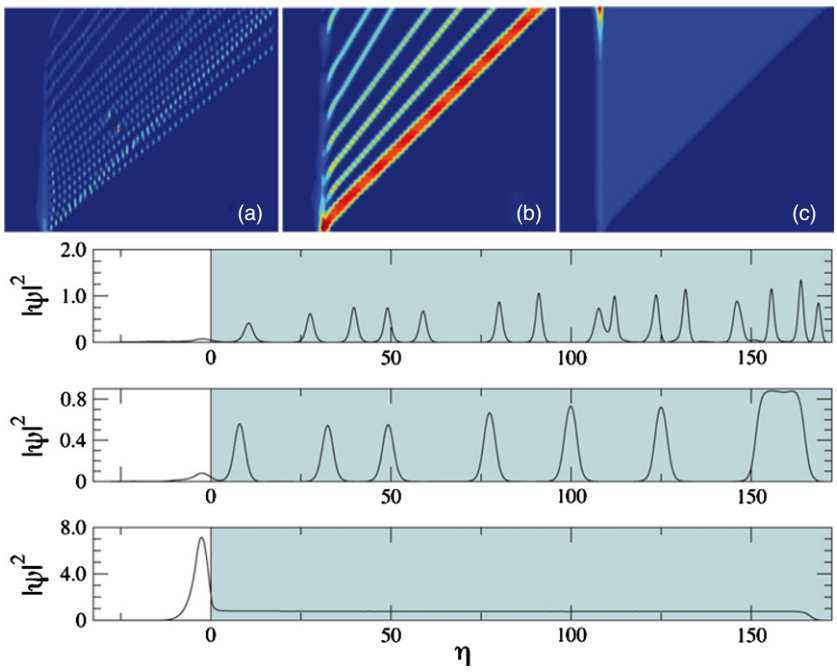

Figure 2. Evolution of a Gaussian atomic cloud in the presence of the localized gain $\Gamma = \Gamma_{cr}$ with the two-body coefficient $\alpha = 1$ and different values of the three-body atomic interactions: (a) $\beta = 0$, (b) $\beta = 0.8$ and (c) $\beta = 1$. In all snapshots, the x-axis displays the spatial coordinate η and the y-axis corresponds to the evolution time $\tau \in [0, 500]$. Shown below are the final density distribution plots of (a) top, (b) middle and (c) bottom figures.

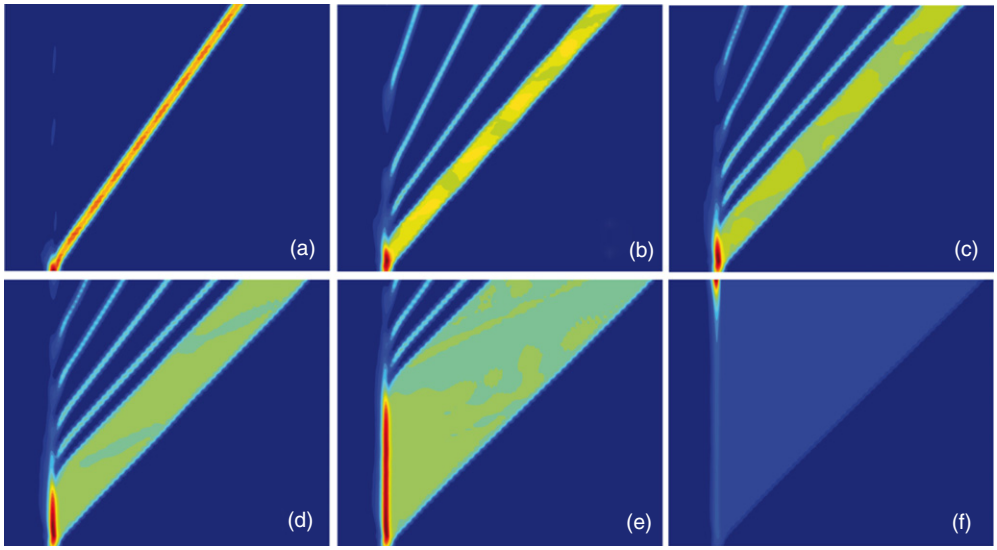

Figure 3. Same as figure 2 for different values of the gain coefficient Γ/Γ_{cr}. In all cases, we have fixed $\alpha = \beta = 1$. In (a) $\Gamma/\Gamma_{cr} = 0$; (b) $\Gamma/\Gamma_{cr} = 0.8$; (c) $\Gamma/\Gamma_{cr} = 0.93$; (d) $\Gamma/\Gamma_{cr} = 0.98$; (e) $\Gamma/\Gamma_{cr} = 0.99$ and (f) $\Gamma/\Gamma_{cr} = 1$.

depends on the parameters of the system (in the simulations of figure 2, we have fixed $\Gamma = 0.0375$ which corresponds to Γ_{cr} for $\alpha = \beta = 1$), the first soliton emitted becomes wider featuring a flat-top profile [30] which is characteristic of systems with CQ nonlinearity (see picture (b) in figure 2). However, if $\beta > 0$ and $\Gamma \geqslant \Gamma_{cr}$, a continuous beam of constant amplitude is outcoupled from the trap (see picture (c) in figure 2). Note that the density plots in figure 2 correspond to the final evolution stages ($\tau = 500$) of simulations (a) top, (b) middle and (c) bottom.

In terms of the physical description given above, it can be stated that whenever $\Gamma > 0$, the system follows the eigenstate structure for growing values of N, but only above the critical value Γ_{cr} the system is able to produce a coherent plane wave of constant amplitude A. Furthermore, we have checked that the amplitude of the continuous matter wave released remains unaltered (unless small scale fluctuations) when three-body losses [32] are taken into account. We have numerically verified that whenever losses are moderate (typically less than $10^{-3}\beta$), their effect can be compensated by increasing the gain in the system. For greater losses, the analysis turns out to be more complicated and a more careful study, beyond the scope of this paper, must be performed.

Another important feature of our system consists of the possibility of controlling the spatial width of the first soliton outcoupled. For a given pair of nonlinear coefficients $[\alpha, \beta]$, this can be achieved by varying the gain coefficient Γ as it can be seen in figure 3. In the snapshot (a) of figure 3, where Γ is zero, almost all atoms are emitted in a coherent pulse of finite width. The increment in the spatial extension of the atomic soliton becomes non-negligible for small variations of the gain parameter in the regime $\Gamma/\Gamma_{cr} \approx 1$ (see pictures (b)–(f) in figure 3). The case for which the rate of atoms loaded exactly compensates losses due to CW emission is illustrated in figure 3(f). It is noticeable that for $\Gamma > \Gamma_{cr}$, the CW emitted preserves its peak density and constant shape, indicating that the method is robust against perturbations.

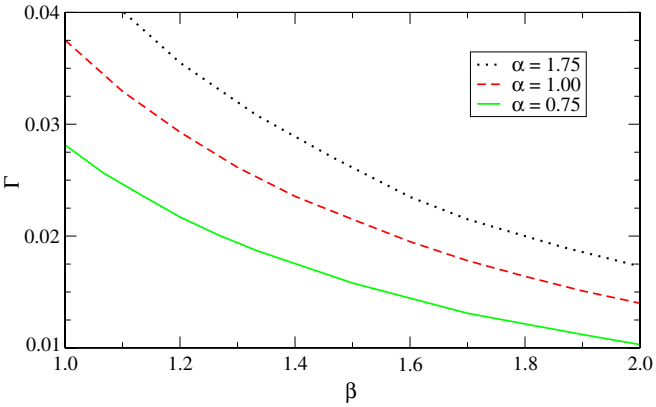

Figure 4. Working range of the CW atomic laser for three different values of the two-body interaction parameter: $\alpha = 1.75$ (black pointed); $\alpha = 1$ (red dashed) and $\alpha = 0.75$ (green continuous). For each value of the three-body interaction coefficient β, the corresponding Γ_{cr} is plotted indicating that over this value CW emission is always achieved.

In figure 4, we have plotted the results of many simulations in the whole parameter space, showing the working range of the CW atom laser for different α values. The plotted lines define the lower border of the operational region for each α, i.e. the line points correspond to $\Gamma = \Gamma_{cr}$, and CW emission is assured for gain values over such limit.

5. Analytic condition for CW emission

In the following, we will derive an analytic expression for the continuous matter wave emission based on waveguide modal theory [33].

We consider the linear trap (depicted in figure 1) as a one-dimensional linear step-index waveguide with the core index $n_c = V_0$, cladding index $n_{cl} = 0$ (left trap border) and substrate index $n_s = V_{nl}$ (right border), V_{nl} being the effective potential

created by the nonlinear interactions. For the moment, we will treat $V_{\rm nl}$ as a constant value. In this context, the guiding properties of the structure can be characterized by both the normalized frequency $f_0 = L\sqrt{V_0 - V_{\rm nl}}$ and the cut frequency $f_c(\nu) = \arctan\sqrt{V_{\rm nl}/(V_0 - V_{\rm nl})} + \nu\pi$, where ν is a non-negative integer, which establishes a cut-off for the existence of guided modes [33]. The specific case $f_c(0)$ corresponds to the threshold of the fundamental mode. We assume that if the lowest energy mode is cut there are no guided modes supported by the waveguide and just radiation modes can be excited. In other words, for $f_0 < f_c(0)$, particles cannot be trapped and will eventually flow towards $\eta > 0$.

Let us determine the values of $V_{\rm nl}$ for which the non-guiding condition $F = f_0 - f_c(0) < 0$ is fulfilled. Fixing L and V_0 to the numbers employed in the simulations, we have found the limiting value $V_{\rm nl}^c = 0.05$ numerically solving $F = 0$. Thus, for $V_{\rm nl} > V_{\rm nl}^c$, the guide cannot retain the matter-wave field, while in the opposite case the particles will remain trapped if the proper mode is correctly excited. Hereafter, we will consider $V_{\rm nl}$ to be field-dependent owing to the existence of nonlinear interactions within the region $\eta \geqslant 0$. On the right border of the dipole trap, $V_{\rm nl}^c = \alpha|\psi|^2 - \beta|\psi|^4$, indicating that the potential barrier depends on the particle density. Note that as $|\psi|^2$ must be real, the latter expression predicts a cut-off in the outcoupling mechanism since for $V_{\rm nl}^c \geqslant \frac{\alpha^2}{4\beta}$, the emission is forbidden. The agreement between analytical and numerical estimations of this cut-off is above 90%.

We have also determined the dependence of $V_{\rm nl}^c$ on V_0 (fixing L) to be linear with the slope $\xi = 0.917$, ordinate $\chi = -0.039$ and correlation $R^2 = 0.9998$. Finally, assuming that the atomic cloud features a Gaussian transverse profile as in the whole simulations, we arrive at the analytic expression for the emission condition:

$$A^2 \geqslant \frac{\alpha + \sqrt{\alpha^2 - 4\beta(\xi V_0 + \chi)}}{2\beta\, \mathrm{e}^{-\frac{L^2}{2\omega^2}}}, \qquad (4)$$

where A is the amplitude of the Gaussian atomic cloud loaded in the trap. This condition establishes a lower limit for matter-wave emission. Continuous operation of the atom laser will be assured by keeping the peak particle density A^2 above this threshold. In our numerical simulations, we have added a linear gain factor in order to satisfy this condition. Experimentally this could be realized by continuously loading the optical trap with a flux of particles [31].

6. Discussion and conclusions

We have shown in this work that CW operation of a matter-wave laser could be realized within an ample parameter space for a negative scattering length and repulsive three-body elastic interactions. Although the cubic–quintic model can be considered an exotic system, it has been proposed that *repulsive* three-body forces can be activated by simultaneously switching on an optical lattice in $\eta \geqslant 0$ containing an ultracold gas of particles with high magnetic or electric dipole moment [19].

In summary, we have proposed a novel mechanism for continuous operation of a coherent matter-wave laser. Our system is able to perform a regular and controllable emission of coherent atomic beams of constant amplitude with the only limitation of the number of particles that can be loaded in the trap. It is important to note that even though the present paper is devoted to square traps, our results also apply to other trap configurations without loss of generality. We have also shown how the width of the first atomic soliton released can be easily controlled by means of the variations of the input gain. Moreover, we have derived an analytic condition for the CW emission which relates the peak particle density of the atomic cloud to the tunable parameters of the system. As the techniques for coherently feeding BECs progress, our idea could provide a novel approach to new types of matter-wave lasers.

Acknowledgments

This work was supported by Ministerio de Educación y Ciencia, Spain (project FIS2008-01001) and University of Vigo (project 08VIA09). D Novoa acknowledges the support from Consellería de Innovación e Industria-Xunta de Galicia through the *María Barbeito* program.

References

[1] Anderson M H, Ensher J R, Matthews M R, Wieman C E and Cornell E A 1995 *Science* **269** 198
Davis K B, Mewes M-O, Andrews M R, van Druten N J, Durfee D S, Kurn D M and Ketterle W 1995 *Phys. Rev. Lett.* **75** 3969
[2] Mewes M-O, Andrews M R, Kurn D M, Durfee D S, Townsend C G and Ketterle W 1997 *Phys. Rev. Lett.* **78** 582
[3] Carr L D and Brand J 2004 *Phys. Rev.* A **70** 033607
[4] Rodas-Verde M I, Michinel H and Pérez-García V M 2005 *Phys. Rev. Lett.* **95** 153903
Carpentier A V, Michinel H and Rodas-Verde M I 2006 *Phys. Rev.* A **74** 013619
[5] Bloch I, Hänsch T W and Esslinger T 1999 *Phys. Rev. Lett.* **82** 3008
[6] Hagley E, Deng L, Kozuma M, Wen J, Helmerson K, Rolston S L and Phillips W D 1999 *Science* **283** 1706
[7] Bloch I, Kšhl M, Greiner M, Hänsch T W and Esslinger T 2001 *Phys. Rev. Lett.* **87** 030401-1
Kohl M *et al* 2002 *Phys. Rev. Lett.* **87** 160404
Kohl M, Hänsch T W and Esslinger T 2002 *Phys. Rev.* A **65** 021606
[8] Martin J L, McKenzie C R, Thomas N R, Warrington D M and Wilson A C 2000 *J. Phys. B: At. Mol. Opt. Phys.* **33** 3919
[9] Mohring B, Bienert M, Haug F, Morigi G and Schleich W P 2005 *Phys. Rev.* A **71** 053601
[10] Guerin W, Riou J-F, Gaeblert J P, Josse V, Bouyer P and Aspect A 2006 *Phys. Rev. Lett.* **97** 200402
[11] Couvert A, Jeppesen M, Kawalec T, Reinaudi G, Mathevet R and Guéry-Odelin D 2008 *Europhys. Lett.* **83** 50001
[12] Gattobigio G L, Couvert A, Jeppesen M, Mathevet R and Guéry-Odelin D 2009 *Phys. Rev.* A **80** 041605
[13] Delgado F, Muga J G and Ruschhaupt A 2006 *Phys. Rev.* A **74** 063618
[14] Robins N P, Savage C M, Hope J J, Lye J E, Fletcher C S, Haine S A and Close J D 2004 *Phys. Rev.* A **69** 051602
[15] Gustavson T L, Bouyer P and Kasevich M A 1997 *Phys. Rev. Lett.* **78** 2046
[16] Pérez-García V M, Michinel H and Herrero H 1998 *Phys. Rev.* A **57** 3837

[17] Strecker K E, Partridge G B, Truscott A G and Hulet R G 2002 *Nature* **417** 150
[18] Khaykovich L, Schreck F, Ferrari G, Bourdel T, Cubizolles J, Carr L D, Castin Y and Salomon C 2002 *Science* **296** 1290
[19] Buchler H P, Micheli A and Zoller P 2007 *Nat. Phys.* **3** 726
[20] Inouye S, Andrews M R, Stenger J S, Mierner H-J, Stamper-Kurn D M and Ketterle W 1998 *Nature* **392** 151
[21] Theis M, Thalhammer G, Winkler K, Hellwig M, Ruff G, Grimm R and Denschlag J H 2004 *Phys. Rev. Lett.* **93** 123001
[22] Sage J M, Sainis S, Bergeman T and DeMille D 2005 *Phys. Rev. Lett.* **94** 203001
[23] Griesmaier A, Werner J, Hensler S, Stuhler J and Pfau T 2005 *Phys. Rev. Lett.* **94** 160401
Ronen S, Bortolotti D C E, Blume D and Bohn J L 2006 *Phys. Rev.* A **74** 033611
[24] Knoop S, Ferlaino F, Mark M, Berninger M, Schöbel H, Nägerl H-C and Grimm R 2009 *Nat. Phys.* **5** 227
Kraemer T *et al* 2006 *Nature* **440** 315
[25] Giovanazzi S, Pedri P, Santos L, Griesmaier A, Fattori M, Koch T, Stuhler J and Pfau T 2006 *Phys. Rev.* A **74** 013621
[26] Stamper-Kurn D M, Andrews M R, Chikkatur A P, Inouye S, Miesner H-J, Stenger J and Ketterle W 1998 *Phys. Rev. Lett.* **80** 2027
[27] Martikainen J P 2001 *Phys. Rev.* A **63** 043602
[28] Jackson A D, Kavoulakis G M and Pethick C J 1998 *Phys. Rev.* A **58** 2417
[29] Piekara A H, Moore J S and Feld M S 1974 *Phys. Rev.* A **9** 1403
[30] Novoa D, Michinel H and Tommasini D 2009 *Phys. Rev. Lett.* **103** 023903
[31] Aghajani-Talesh A, Falkenau M, Griesmaier A and Pfau T 2009 *J. Phys. B: At. Mol. Opt. Phys.* **42** 245302
[32] Kagan Yu, Muryshev A E and Shlyapnikov G V 1997 *Phys. Rev. Lett.* **81** 933
[33] Tamir T 1979 *Integrated Optics* (Berlin: Springer)